Cell Mol Neurobiol (2015) 35:57–70
DOI 10.1007/s10571-014-0145-7

ORIGINAL RESEARCH

Time Course of Spinal Doublecortin Expression in Developing Rat and Porcine Spinal Cord: Implication in In Vivo Neural Precursor Grafting Studies

J. Juhasova · S. Juhas · M. Hruska-Plochan · D. Dolezalova · M. Holubova · J. Strnadel · S. Marsala · J. Motlik · M. Marsala

Received: 25 April 2014 / Accepted: 19 November 2014 / Published online: 9 December 2014

Abstract Expression of doublecortin (DCX), a 43–53 kDa microtubule binding protein, is frequently used as (i) an early neuronal marker to identify the stage of neuronal maturation of in vivo grafted neuronal precursors (NSCs), and (ii) a neuronal fate marker transiently expressed by immature neurons during development. Reliable identification of the origin of DCX-immunoreactive cells (i.e., host vs. graft) requires detailed spatial and temporal mapping of endogenous DCX expression at graft-targeted brain or spinal cord regions. Accordingly, in the present study, we analyzed (i) the time course of DCX expression in pre- and postnatal rat and porcine spinal cord, and (ii) the DCX expression in spinally grafted porcine-induced pluripotent stem cells (iPS)-derived NSCs and human embryonic stem cell (ES)-derived NSCs. In addition, complementary temporospatial GFAP expression study in porcine spinal cord was also performed. In 21-day-old rat fetuses, an intense DCX immunoreactivity distributed between the dorsal horn (DH) and ventral horn was seen and was still present in the DH neurons on postnatal day 20. In animals older than 8 weeks, no DCX immunoreactivity was seen at any spinal cord laminae. In contrast to rat, in porcine spinal cord (gestational period 113–114 days), DCX was only expressed during the pre-natal period (up to 100 days) but was no longer present in newborn piglets or in adult animals. Immunohistochemical analysis was confirmed with a comparable expression profile by western blot analysis. Contrary, the expression of porcine GFAP started within 70–80 days of the pre-natal period. Spinally grafted porcine iPS-NSCs and human ES-NSCs showed clear DCX expression at 3–4 weeks post-grafting. These data indicate that in spinal grafting studies which employ postnatal or adult porcine models, the expression of DCX can be used as a reliable marker of grafted neurons. In contrast, if grafted neurons are to be analyzed during the first 4 postnatal weeks in the rat spinal cord, additional markers or grafted cell-specific labeling techniques need to be employed to reliably identify grafted early postmitotic neurons and to differentiate the DCX expression from the neurons of the host.

Keywords Doublecortin · Spinal cord development · Spinal neural precursor grafting · Minipig · Rat · GFAP

J. Juhasova · S. Juhas (✉) · J. Motlik
Laboratory of Cell Regeneration and Plasticity, Institute of Animal Physiology and Genetics, AS CR, v.v.i., Rumburska 89, 27721 Libechov, Czech Republic
e-mail: juhas@iapg.cas.cz

M. Hruska-Plochan · D. Dolezalova · J. Strnadel · S. Marsala · M. Marsala
Department of Anesthesiology, University of California, San Diego, La Jolla, CA, USA

M. Hruska-Plochan
Institute of Molecular Life Sciences, University of Zurich, Zurich, Switzerland

D. Dolezalova
Department of Histology and Embryology, Faculty of Medicine, Masaryk University, Brno, Czech Republic

M. Holubova · J. Strnadel
Laboratory od Tumor Biology, Institute of Animal Physiology and Genetics, AS CR, v.v.i., Rumburska 89, 27721 Libechov, Czech Republic

Introduction

Several previous experimental studies have demonstrated the successful utilization of mouse, rat, or human neural or neuronal precursors for brain or spinal cord grafting using a

variety of neurodegenerative models. Depending on the origin of grafted cells (i.e., rodent, porcine, or human origin) and the animal species of the recipient, the strategies to identify grafted cells can be divided into several categories (i) labeling of grafted cells with chemical-fluorescent surface or cytoplasmic markers (Cao et al. 2008; Wallace and Muirhead 2007), (ii) labeling of mitotically active precursors before grafting with BrdU or with lentivirus or adeno-associated virus encoding fluorescent reporter gene(s) (Tabar et al. 2005; Cizkova et al. 2006; Marsala et al. 2004), (iii) utilization of cells derived from transgenic animals expressing neuron-specific or non-specific fluorescent reporters or human-specific placental alkaline phosphatase (Hakamata et al. 2001; Inoue et al. 2005; Okabe et al. 1997; Lepore and Fischer 2005; Kawaguchi et al. 2001), and (iv) the use of human neural or neuronal precursors and identification of grafted cells with human-specific antibodies which do not cross-react with the graft recipient (Kakinohana et al. 2004; Cizkova et al. 2007; Marsala et al. 2004; van Gorp et al. 2013; Lu et al. 2012).

In addition to direct labeling techniques or use of human-specific antibodies to identify grafted cells, a separate category is represented by utilization/identification of markers which are only transiently expressed in grafted cells but are not present in the host tissue. Among these, nestin and doublecortin (DCX) staining is most frequently used to identify grafted neural precursors or early postmitotic neurons, respectively. DCX is a 43–53 kDa microtubule binding protein which regulates the stability of microtubules and plays an important role in neuronal migration and proper cortical neuronal layering during development (Karl et al. 2005; Magavi and Macklis 2008). In adult rodent brain, continuing expression of DCX in early postmitotic/migrating neurons in neurogenic zones (Couillard-Despres et al. 2008; Couillard-Despres et al. 2005; Hua et al. 2008; Nacher et al. 2001) was also reported. In addition to brain, DCX is also expressed in spinal cord during early stages of development but is absent in the intact or traumatically injured adult rat spinal cord (Johansson et al. 1999; Gleeson et al. 1999; Couillard-Despres et al. 2005; Sabelström et al. 2014).

Consistent with the transient nature of DCX expression in developing brain or spinal cord neurons, a similar transient DCX expression in vitro cultured early postmitotic neurons (Jin et al. 2002; Walker et al. 2007) or neuronal precursors/postmitotic neurons grafted into rodent brain or spinal cord injury models was reported (Darsalia et al. 2007; Englund et al. 2002). These studies, for example, show that grafted neural stem cells (NSCs) may partly improve impaired neurological functions in stroke-subjected animals. In the transplantation core, cells were undifferentiated and expressed markers of immature neural lineage as nestin and, to a lesser extent, also GFAP, beta III-tubulin, DCX, and calretinin. In contrast, cells localized at the periphery of grafts exhibited mature neuronal morphology and expressed mature neuronal markers such as HuD, calbindin, and parvalbumin (Darsalia et al. 2007).

Similarly, selective DCX expression in grafted human fetal brain tissue-derived neurons was demonstrated (Kelly et al. 2004). In our previous studies, we have demonstrated that a subpopulation of spinally grafted human spinal stem cells when grafted at the nestin-positive stage continue to express DCX at 3 months when grafted into previously ischemia-injured spinal cord segments (Cizkova et al. 2007). Similarly, we have demonstrated a comparable level of DCX expression in human spinal stem cells at 6–7 weeks after spinal grafting in adult immunosuppressed naive minipigs (Usvald et al. 2010) or in human embryonic stem cell-derived NSCs at 2 weeks–3 months after grafting into lumbar spinal cords of naive or ALS ($SOD1^{G93A}$) immunosuppressed rats (Sevc et al. 2013).

Despite the relatively extensive use of DCX as an early neuronal marker of grafted neurons, a detailed characterization of DCX expression in spinal cord during the pre-natal and early postnatal period in relevant experimental animal species is not available. Such data are critical to permit the reliable interpretation of DCX expression in grafted neurons derived from animal models or human neurons and to dissociate such expression from the host.

Accordingly, in the present study, we characterize the time course of spinal expression of DCX during the pre- and postnatal period in SD rats and Gottingen-Minnesota minipigs. In addition, the DCX expression profile in spinally grafted porcine iPS-derived NSCs or human ES-NSCs in immunodeficient rats or immunosuppressed minipig was studied. Finally, the expression of GFAP during the pre- and postnatal period in Gottingen-Minnesota minipigs was also analyzed.

Materials and Methods

Minipig and Rat Fetal Tissue Isolation

General anesthesia was induced in (i) minipig pregnant females ($n = 8$) at 40, 60, 80, 100, 110 days, and in (ii) adult minipigs ($n = 3$) by intramuscular application of TKX mixture (Tiletaminum 5 mg/kg, Zolazepamum 5 mg/kg, Ketaminum 5 mg/kg, Xylazine 1 mg/kg). Similarly, in pregnant Wistar rat dams or adult rats, terminal anesthesia was induced by intraperitoneal administration of thiopental at a dose of 70 mg/kg of body weight. After induction of anesthesia, a total abdominal hysterectomy was performed and all available embryos were rapidly (3–5 min) removed, washed in sterile phosphate buffered

saline (PBS) and animals were divided into two groups (IHC analysis and WB analysis).

Perfusion Fixation and Spinal Cord Tissue Harvest

In 21-day-old rat fetuses, 3- and 5-day-old rats as well as 40-day-old porcine fetuses, the spinal cord was dissected on ice and then fixed in situ in 4 % paraformaldehyde for 2–3 days at 4 °C. In 60-, 70-, 80-, 100- or 110-day-old porcine fetuses, the chest cavity was opened and animals perfused through the descending thoracic aorta with heparinized ice-cold saline (300 ml) followed by 4 % paraformaldehyde (PFA; 300 ml). Spinal cords were then dissected and postfixed for 24 h in the same fixative before tissue processing. Adult rats (3 months old; $n = 3$) and minipigs (3 months old; $n = 3$) were transcardially perfused with heparinized saline followed by 4 % PFA. After postfixation tissue was cryoprotected in 30 % sucrose with sodium azide. Transverse sections of lumbar, thoracic, and cervical spinal cord were cut on a freezing microtome (CM1850; Leica Microsystems) at 20–40-μm thicknesses, and stored in PBS at 4 °C. An identical perfusion fixation procedure was performed in immunodeficient rats or immunosuppressed minipigs previously grafted with human ES-NSCs or porcine iPS-NSCs.

Western Blot Analysis of DCX and GFAP in Rat and Porcine Spinal Cord and Cells

Rat and miniature pig spinal cords without PFA fixation were cryo-sectioned. A collection of fifty sections (10 μm) was lysed for 30 min using lysis buffer containing 50 mM Tris (pH 7.4) (5429.3; Roth), 250 mM NaCl (3957.2; Roth), 5 mM EDTA (E5134; Sigma), 50 mM NaF (S-1504; Sigma), 1 mM Na_3VO_4 (S6508; Sigma) in 1 % Triton® X-100 (T8532; Sigma) with protease inhibitor cocktail tablets (Complete Mini, EDTA-free; 11836170001; Roche), and 1 mM phenylmethylsulphonyl fluoride (PMSF; 837091; Roche). The pellets of rat and pig fibroblasts as well as pig NSCs were directly lysed in the lysis buffer mentioned above. Sonications of all samples were performed in a cold water bath for 5 min and followed by centrifugation at 10,000*g* at 4 °C for 20 min. Total protein levels were determined by BCA Protein Assay Kit (#23225, ThermoScientific) and 15 micrograms of each sample was loaded on the 10 % gel acrylamide gels together with sample buffer (125 mM Tris–HCl, 4 % SDS, 20 % glycerol, 10 % 2-mercaptoethanol, 0.004 % bromophenol blue) and distilled water. After polyacrylamide gel electrophoresis, the proteins were transferred to nitrocellulose membranes using a semidry blotting system. The membranes were blocked with 5 % nonfat dry milk (NFDM) in tris-buffered saline with 0.5 % Tween 20 (TBS-T). The membranes were incubated with the primary antibodies, goat polyclonal antibody anti-doublecortin (Santa Cruz, sc-8066, diluted 1:200), or mouse monoclonal anti-GFAP antibody (Sigma, C9205, 1:2000) in 5 % NFDM in TBS-T overnight on roller at 4 °C. After washing with TBS-T buffer, the membrane was consequently incubated in donkey anti-goat or donkey anti-mouse Ab HRP conjugate (Jackson Labs) diluted 1:10 000 in 5 % NFDM in TBS-T 1 h at RT with gentle shaking. A Super-Signal West Pico Chemiluminescent Substrate (34077, Pierce) detection system was used for visualization. Western blotting signal was quantified by determining the gray values of given bands using the ImageJ software.

Preparation of Human Embryonic Stem Cell-Derived and Pig-Induced Pluripotent Stem Cell-Derived Neural Precursors

Human ES-NPC Preparation

Colonies of hESCs lines (UCSF4.3) were manually dissociated into smaller clumps and induced to form embryoid bodies (EBs) in the presence of DMEM/F12 media supplemented with supplemented with 15 % knockout serum replacement, 2 mmol/l L-Glutamine, 1× minimum essential medium (MEM) non-essential amino acids, (all media components from Life Technologies, Carlsbad, CA, USA), and 100 μmol/l β-2 mercaptoethanol (Sigma-Aldrich, St. Louis, MO, USA). After 4–6 days, EBs were transferred onto cell culture dishes freshly coated with Poly-L-Ornithine (Sigma-Aldrich) and Laminin (Life Technologies; P/L) and allowed to adhere for 48 h in NSC media (DMEM/F12, 0.5xN2 media supplement, 0.5xB27 media supplement (Life Technologies), 2 mmol/l L-Glutamine, and 20 ng/ml FGF-2 (Millipore, Billerica, MA, USA). Formation of neural rosettes was observed at days 4–12 after plating. Neural rosettes were manually separated under the dissection microscope, dissociated into smaller pieces, and transferred to new P/L coated cell culture dishes. Upon adhesion, dissected clumps of rosettes began to generate new groups of rosettes as well as independent homogenous clusters of radially organized columnar epithelial cells adjacent to major areas of rosettes. These populations of NSCs were manually separated onto new culture plates coated with P/L and grown in the presence of NSC media. Upon reaching confluency, NSCs were enzymatically passaged using 0.05 % Trypsin and subsequently 1x Defined Trypsin Inhibitor (Life Technologies). Established lines displayed consistent expression of markers typical for NSCs (>75 % of Nestin, Sox1, Sox2 and Pax6 expression) and no residual expression of pluripotency transcription factor Nanog. For in vivo spinal grafting, proliferating non-induced NSCs were used.

Pig iPS-NPC Preparation

Fibroblast culture was established from ear skin punch of 6-weeks-old piglets and transduced with integrating (retrovirus) and non-integrating (Sendai virus) vectors encoding Oct4, Sox2, Klf4, and c-myc, as previously described (Marchetto et al. 2010). Derived iPS colonies were maintained on a feeder layer of mitotically inactivated mouse embryonic fibroblasts (MEFs) and passaged manually by selection of individual iPS colonies using an EVOS scope. To induce NSCs from iPS cells, the colonies were transferred to low attachment surface plates and induced with DMEM/F12, N2 and 5 μM Dorsomorphin. After plating in matrigel coated plates, rosette-like structures were harvested, expanded in the presence of bFGF (10 ng/ml), and purified by (a) feeder cell removal using magnetic sorting (Miltenyi Biotech), (b) positive magnetic sorting for the PSA-NCAM+ population (Miltenyi Biotech), and (c) FAC-sorting and selection of CD184+/CD24+/CD271(−) NSCs population (Yuan et al. 2011). Sorted cells were further expanded using the bFGF (10 ng/ml) as a solo mitogen. For in vivo spinal grafting, proliferating non-induced NSCs were used.

In Vivo Spinal Human ES-NPC and Pig iPS-NPC Grafting

Spinal Human ES-NSC Grafting in Immunodeficient Rats

Immunodeficient rats were anesthetized with 1.5–2 % isoflurane, placed into a spinal unit apparatus (Stoelting, Wood Dale, IL, USA) and a partial dorsal laminectomy of Th12-L1 vertebra was performed using a dental drill (exposing the dorsal surface of L2–L5 spinal segments). Using a glass capillary connected to a microinjector (Stoelting), rats received 10 bilateral injections of the ES-NSCs (5 on each side; 0.5 μl/injection; 15,000–20,000 cells/μl; $n = 3$) in hibernation buffer. The duration of each injection was 60 s followed by a 30-s pause before capillary withdrawal. The center of the injection was targeted into the central gray matter (laminae V–VII) (distance from the dorsal surface of the spinal cord at L3 level: 1 mm) (Kakinohana et al. 2004). The rostrocaudal distance between individual injections ranged between 300 and 500 μm. After implantation, the incision was cleaned with 3 % H_2O_2 and penicillin/streptomycin mixture and closed in two layers. All animals were perfusion fixed with 4 % paraformaldehyde at 3 weeks after cell grafting.

Spinal Pig iPS-NPC Grafting in Immunosuppressed Pigs

Adult Yucatan female minipigs (25–30 kg; $n = 3$) were prepared for spinal cell grafting as previously described (Usvald et al. 2010). Briefly, minipigs were premedicated with intramuscular azaperonum (2 mg/kg) and atropine (1 mg/kg; Biotika, SK) and then induced with ketamine (20 mg/kg, i.v.). After induction, animals were intubated with a 2.5F tracheal tube. Anesthesia was maintained with 1.5 % isoflurane. Oxygen saturation was monitored throughout the procedure using a pulse oximeter (Nellcor Puritan Bennett Inc., Ireland). After induction of anesthesia, animals were placed into supine position with all 4 extremities fixed to the operating table. The left jugular vein was exposed and catheterized with an 18G central venous catheter (Certofix Mono V 330; B Braun, Germany). The end of the catheter was externalized on the side of the neck. Animals were then placed into prone position and prepared for spinal cell grafting. To immobilize the lumbar spinal cord, animals were mounted into a spinal immobilization apparatus and the lumbar portion of the animal was lifted 5″ above the operating table to eliminate respiration-caused spinal cord pulsation (Dolezalova et al. 2014). A dorsal laminectomy of L2–L5 vertebrae, corresponding to L3–L6 spinal segments, was then performed and epidural fat removed using cotton swabs. The dura was left intact. To deliver cells, the XYZ manipulator (Stoelting, Wood Dale, IL, USA) was used and mounted directly to the operating table. A Hamilton syringe with a 30 gauge needle was then mounted into the manipulator and connected to the microinjector (Stoelting) using PE-50 tubing. To connect the PE-50 tubing to the Hamilton syringe, the plunger was removed and one end of the PE-50 tubing was inserted 1 cm into the syringe and sealed with silicone. Animals then received a total of 10 injections of porcine iPS-NSCs (5 on each side; 6 μl/injection; 15,000–20,000 cells/μl) targeted into the intermediate zone (lamina VII) of L3-L6 segments. The distance between individual injections was 1–1.5 mm. All surgical interventions followed rigid aseptic procedures. All materials were subjected to autoclaving or gas sterilization.

Immediately after jugular vein catheterization the animals received a bolus (0.1 mg/kg) injection of Prograf® followed by a continuous Prograf infusion (0.05 mg/kg/day) using externally mounted 5–7 day infusion pumps (Baxter Infusor) secured in a custom-made "minipig jacket". After cell grafting, animals survived for 6 weeks and were then transcardially perfused using 4 % paraformaldehyde.

Imunohistochemistry of Spinal Cord Sections

For single as well as double immunostaining of spinal cord sections a nonspecific binding was blocked for 1 h at RT with 1 % bovine serum albumin (Albumin bovine Fraction V; 11922; SERVA) in 0.2 % Triton-X PBS. Free-floating or glass-mounted sections were sequentially stained with anti-doublecortin primary antibody (goat polyclonal IgG; 1:500; sc-8066; Santa Cruz Biotechnology; rabbit

polyclonal IgG, 1:400, #4604, Cell Signaling Technology; mouse monoclonal, clone 3E1, IgG2a,k,1:500, LS-C204512, LifeSpan BioSciences, Inc.), anti-GFAP antibody (mouse monoclonal Anti-Glial Fibrillary Acidic Protein (GFAP)-Cy3™ antibody; 1:2000; C9205; Sigma), anti NeuN antibody (mouse monoclonal; MAB377; 1:1000; Chemicon), or anti Vimentin antibody (1:1000, ABCAM) in 0.2 % Triton-X PBS for 72 h at 4 °C. For confirmation of sc-8066 antibody specificity, we used an adsorption control by incubation of sc-8066 antibody with sc-8066P peptide (1:10 ratio) for 24 h at 4 °C before applying on the sample. In rats grafted spinally with human ES-NSCs, a human-specific nuclear antibody (hNUMA; 1:100, Millipore) was used to identify grafted cells of human origin.

After incubation with primary antibodies, sections were developed using biotinylated or fluorescent secondary antibodies (Donkey anti-rabbit, RPN 1004V, 1:400, GE Healthcare Life Sciences; Sheep anti-mouse, RPN 1001V, 1:400, GE Healthcare Life Sciences; Alexa Fluor® 488 donkey anti-goat IgG, A-11055, 1:500; Alexa Fluor® 488 goat anti-mouse IgG (H+L), A-11001, 1:500; Alexa Fluor® 555 goat anti-mouse IgG, A-21424, 1:500, Invitrogen) in 0.2 % Triton-X PBS for 1.5 h at room temperature. Avidine-peroxidase (A3151; Sigma-Aldrich) complex was visualized by DAB tablet (SIGMAFAST™, D4418). Slides were analyzed and imaged on an epifluorescence microscope (AX70; Olympus), virtual slide scanning system (VS120FL, Olympus) and a confocal microscope (TCS SP5; Leica Microsystems).

Results

Transient DCX Expression Occurs in Rat But Not in Pig Spinal Cord After Birth

Pig Spinal Cord

Immunohistochemistry of spinal cord sections with anti-DCX antibodies revealed a high DCX immunoreactivity (IR) in the entire transverse spinal cord section of the porcine fetal lumbar spinal cord at day 40 (Fig. 1A–A‴, Fa, Ga, Ga′). Intensely stained DCX positive nerve processes surrounding NeuN positive neurons were also identified (Fig. 1A′, A″). In the ventral horn, the highest DCX IR was identified in centrally located developing α-motoneurons (Fig. 1A″, A‴; yellow circles) while the medial and lateral α-motoneuronal group showed minimal or no DCX IR (Fig. 1A″, A‴; white circles).

Analysis of DCX expression in a 60-day-old fetus showed remaining DCX expression in the subpopulation of the dorsal horn (DH) neurons localized between laminae II–V (Fig. 1B, B′). Many scattered double IR immature DCX/NeuN+ neurons with unipolar, or bipolar processes (Fig. 1B′, B″) and localized in the vicinity of large or medium sized NeuN (red) positive, more mature neurons were identified in the deeper laminae of the DH in zona intermedia and ventral horn (Fig. 1B″, B‴, B⁗).

Similar pattern of spinal DH DCX expression, as seen at 60 days, was seen in an 80-day-old-fetus. There was a gradual decrease in DCX IR in deeper laminae (Laminae VIII and IX) (Fig. 1C, C″, Gb, Gb́). However, many multipolar immature DCX neurons with highly branched dendritic processes co-expressing NeuN positivity were found in the zona intermedia (lamina VII) as well as in the ventral horn in laminae VIII and IX (Fig. 1C′- C‴).

Analysis of spinal DCX IR in a 100-day-old fetus showed persisting DCX positivity in a small subpopulation of DH neurons in laminae I–III. Deeper spinal laminae and the entire ventral horn were free of any DCX+ neurons (Fig. 1D, D′, E, Fc, Gc–c″). Three different DCX antibodies were used to analyze the DCX spinal expression pattern in rostro-caudal direction. Using goat polyclonal anti-DCX antibody (sc-8066), which specificity we confirmed by adsorption control as well as western blot analysis, we revealed a decrease of DH DCX IR from lumbar to cervical spinal cord at 100-day-old fetal stage (Fig. 1E, É).

In newborn piglets (2–3 days old; data not shown) or in an adult minipigs (2–3 months of age; Fd), no DCX IR was seen.

Rat Spinal Cord

Immunofluorescence analysis of DCX IR in rat fetal lumbar spinal cord at day 21 showed high DCX IR between laminae I–VII (Fig. 2A). The DH laminae I–IV as well as deeper laminae (V–VII) contained intensely stained DCX positive nerve processes and double IR DCX/NeuN+ neurons. In the ventral horn, large α-motoneurons were DCX negative while some small interneurons continue to have an intense DCX IR (Fig. 2A′; yellow arrow).

On postnatal day 5, the number of DCX+ neurons decreased in the deep DH and in the intermediate zone (Fig. 2B). However, a high density of DCX+ neurons were still seen in the medial portion of laminae I–III and lamina VII as well as in the descending corticospinal tract (CST) (Fig. 2B, B′; white arrows). Large α-motoneurons in the ventral horn were DCX negative (Figs. 2B″; white arrows). Only occasional DCX+ interneurons were seen in the vicinity of NeuN+ α-motoneurons (Figs. 2B″).

Further decline of DCX expression was seen in the ventral horn and in zona intermedia in rat postnatal spinal cord at day 20 (Fig. 2C–C″). In contrast, a relatively high DCX positivity in the DH neurons in laminae I–II and in the CST located in the white matter (Fig. 2C′, C″; white arrows) was still present.

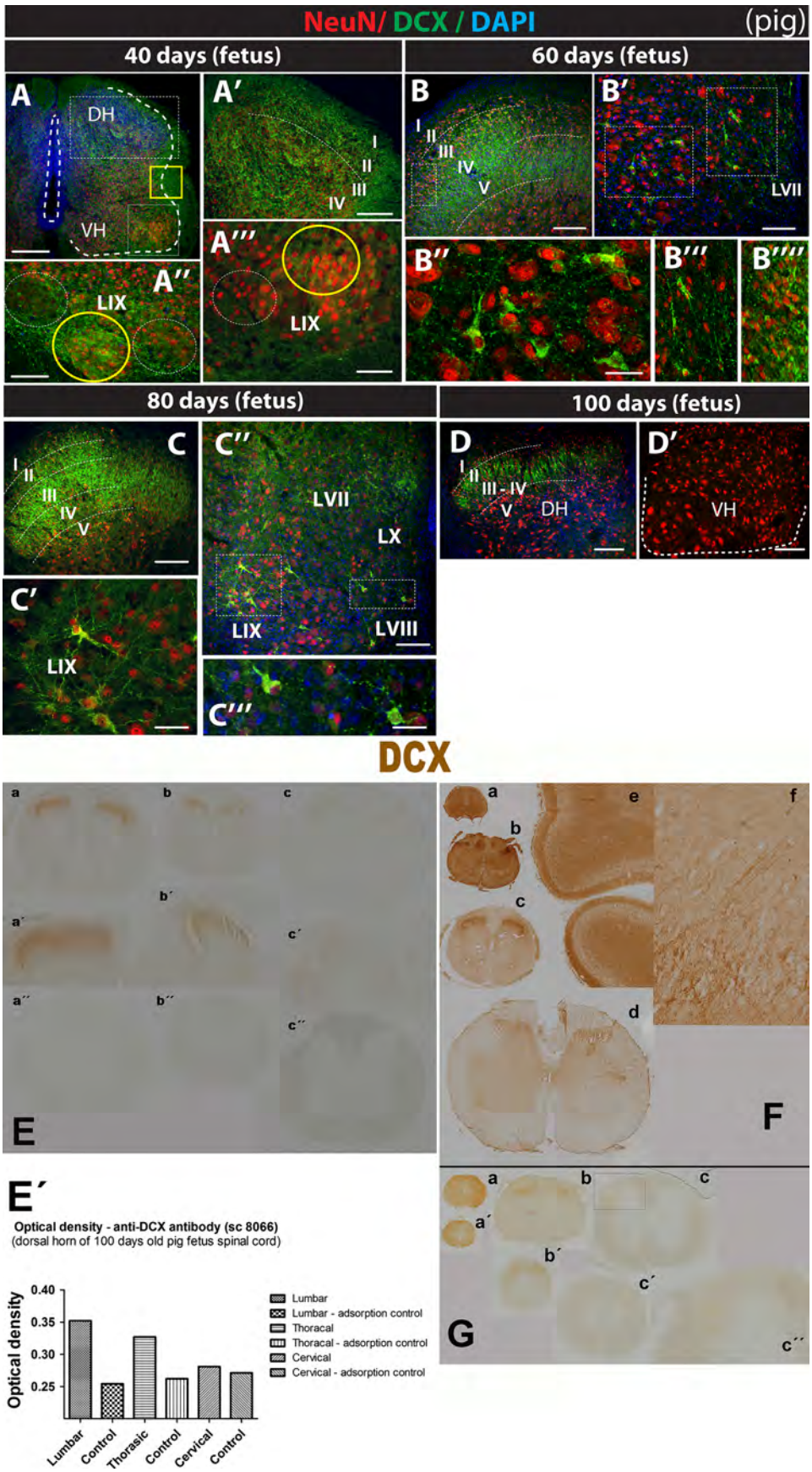
NeuN/ DCX / DAPI (pig)
40 days (fetus)
60 days (fetus)
A
DH
VH
A′
I
II
III
IV
A″
LIX
A‴
LIX
B
I
II
III
IV
V
B′
LVII
B″
B‴
B⁗
80 days (fetus)
100 days (fetus)
C
I
II
III
IV
V
C′
LIX
C″
LVII
LX
LIX
LVIII
C‴
D
I
II
III - IV
V
DH
D′
VH
DCX
E
F
G
E′
Optical density - anti-DCX antibody (sc 8066)
(dorsal horn of 100 days old pig fetus spinal cord)
Optical density
0.40
0.35
0.30
0.25
Lumbar
Control
Thorasic
Control
Cervical
Control
Lumbar
Lumbar - adsorption control
Thoracal
Thoracal - adsorption control
Cervical
Cervical - adsorption control

◀**Fig. 1** DCX expression in developing porcine spinal cord. **A**–**A‴** Transverse spinal cord section taken from 40-day-old porcine fetus and stained with DCX and NeuN antibody. An intense DCX-IR in the majority of neurons in the dorsal and ventral horn can be seen (**A**–**A‴**; *white boxes*). Comparable DCX expression in the lateral funiculus was identified (**A**; *yellow box*). **B**–**B‴**, **C**–**C‴** In 60-80-day-old fetuses, a progressive loss of DCX positive neurons in the ventral (C′) and central gray matter can be seen (**B′**–**B‴**, **C‴**). In contrast, an intense DCX expression continues to be present in the dorsal horn (**B**, **B‴**, **C**) and in a subpopulation of neurons localized in the medial regions of lamina VII (**C″**, **C‴**). **D**–**D′** At 100 days (fetal period), only residual DCX positive neurons localized in laminae I–II can be identified (**D**). DCX immunoreactivity was absent in the deeper laminae (LV–LVII), in the ventral horn and in the *white matter* (**D′**). *Scale bars*: **A** = 1000 μm; **A′**, **B**, **C**, **D**, **D′** = 500 μm; **A″**, **B′**, **C″** = 200 μm; **A‴**, **C′**, **C‴** = 100 μm. *DH* dorsal horn, *VH* ventral horn. **E** Immunohistochemical staining (*brown DAB reaction*) of doublecortin by goat polyclonal anti-DCX (sc-8066) antibody in 100-day-old fetal spinal cord. Lumbar spinal cord (*a*), lumbar spinal cord—dorsal horn detail (*a′*), lumbar spinal cord—adsorption control (*a′*). Thoracic spinal cord (*b*), thoracic spinal cord—dorsal horn detail (*b′*), thoracic spinal cord—adsorption control (*b′*). Cervical spinal cord (*c*), cervical spinal cord—dorsal horn detail (*c′*), cervical spinal cord—adsorption control (*c′*). Magnification x10 (*a*, *a′*, *b*, *b′*, *c*, *c′*), ×66 (*b′*, *c′*), ×100 (*a′*). **E′** Rostro-caudal increase of dorsal horn DCX positivity at 100-day-old fetal spinal cord detected by sc-8066 antibody. **F** Immunohistochemical staining (*brown DAB reaction*) of doublecortin by rabbit polyclonal anti-DCX (#4604) antibody in 40 (*a*), 70 (*b*), 100 (*c*) days old fetal and 3 months old postnatal (*d*) lumbar pig spinal cord. 80-day-old fetal (*e*) and newborn (*f*) cortex were used as a positive controls. 40 and 70-day-old fetal spinal cord showed strong DCX expression. In 100-day-old fetal spinal cord, the maximum DCX immunopositivity was localized in dorsal horn and only weak unspecific signal was present in gray matter of 3 months old postnatal spinal cord. Magnification ×8 (*a*, *b*, *c*, *d*), ×20 (*e*), ×200 (*f*). **G** Immunohistochemical staining (*brown*) of doublecortin by mouse monoclonal anti-DCX (LS-C204512) antibody at 40 (*a*, *a′*), 70 (*b*, *b′*), 100 (*c*, *c′*, *c′*) days old fetal lumbar (*a*, *b*, *c*, *c′*) and thoracic (*a′*, *b′*, *c′*) pig spinal cord. DCX positivity in 100-day-old fetal spinal cord was only observed in dorsal horn (*c′*). Magnification ×10 (*a*, *a′*, *b*, *b′*, *c*, *c′*), ×66 (*c′*)

In animals older than 8 weeks DCX IR was absent in the white or gray matter (data not shown).

DCX Western Blot Analysis

Western Blot analysis of spinal DCX expression at different stages of spinal cord development in rats and pigs showed a similar profile as seen in immunohistochemistry analysis of spinal cord sections. Strong DCX specific bands were detected in the whole miniature pig spinal cord of 40-day-old fetuses. The expression of DCX was stronger in the miniature pig brain in comparison with spinal cord at this fetal stage (data not shown). In 70-day-old minipig fetuses, only moderate expression of DCX was present. No DCX specific bands on day 110 fetal stage or in adult animals were seen (Fig. 2F).

In rats, a progressive decrease in DCX expression was identified in 5-day-old pups and was no longer detectable in the adult rats (Fig. 2F). For confirmation of goat polyclonal anti-DCX antibody (sc-8066) specificity, we also used pig and rat fibroblast (DCX negative control) and pig NSCs (DCX positive control).

GFAP+ Astrocytes Start to Repopulate Fetal Porcine Spinal Cord at 80 Days

Pig Spinal Cord

In the minipig fetus (40 day fetal stage), no GFAP expression was detected in any part of the lumbar spinal cord by immunofluorescence staining or by Western blotting (Fig. 3A, A′, F).

In an 80-day-old fetus, GFAP expression was only seen in the subpial spinal cord regions and was expressed as the presence of radial type of GFAP+ astrocytes with high density processes projecting toward the white matter (Fig. 3B, B′; inset).

In a 100-day-old fetus, the immunofluorescent staining showed a near complete repopulation of the white matter by GFAP+ astrocytes with intense GFAP staining seen in both dorsal and ventral white matter funiculi (Fig. 3C, C′). However, only a relatively weak GFAP IR was seen in the gray matter in dorsal and ventral horn (Fig. 3C, C′; white asterisks).

On the 1st postnatal day, the pattern of GFAP staining was similar as seen at fetal day 100. However, more intense GFAP staining with clearly detectable clusters of GFAP+ processes penetrating into the gray matter was identified. In addition, intense GFAP IR surrounding the areas of lamina X (i.e., around the central canal) was detected (Fig. 3D, D′). In an adult pig (5 months of age), a dense GFAP+ network was found in both white and gray matter (Fig. 3E).

Consistent with immunofluorescence staining data, the Western Blot analysis using GFAP antibody showed the first appearance of GFAP (analyzed in separate cervical, thoracic and lumbar spinal cord samples) in ***A 70-day-old fetus and was increased on 1st postnatal day (Fig. 3F).

Rat Spinal Cord

In a 1-day-old (postnatal) rat, the immunofluorescence staining of transverse lumbar spinal cord sections with GFAP antibody showed the presence of radial type of GFAP astrocytes localized in the subpial regions. No GFAP IR was seen in the deeper regions of the white matter or in the gray matter. In the same regions, intense Vimentin IR was also seen (Fig. 2D–D″). In an adult 3-month-old rat, complete repopulation of gray and white matter with GFAP+ astrocytes was seen (Fig. 2E).

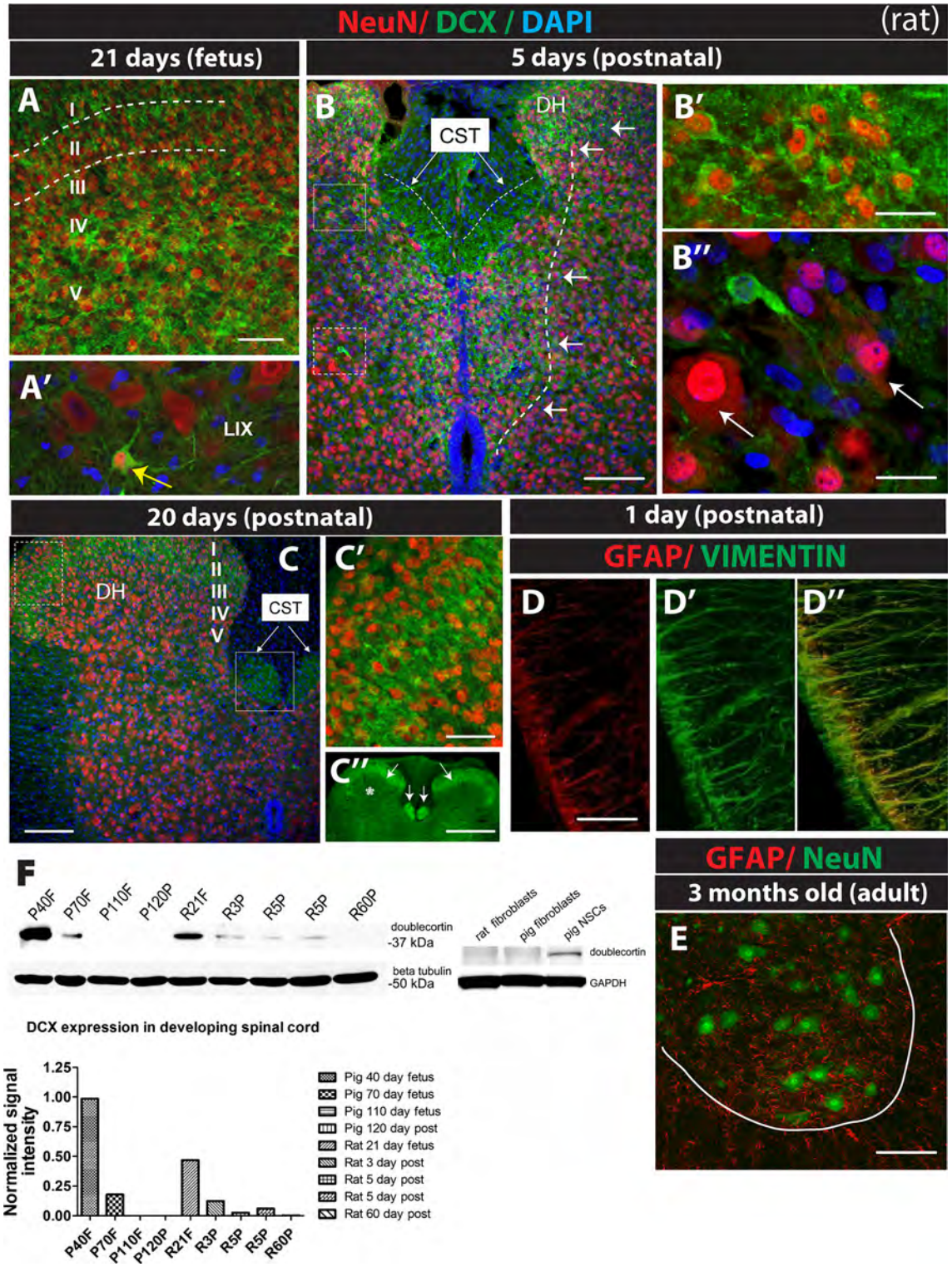

DCX Expression in Spinally Grafted Human Embryonic Stem Cell- and Porcine iPS-Derived Neural Precursors

A grafted cell-specific DCX expression in human ES-NSCs was seen at 3 weeks after grafting into the lumbar spinal cord of naïve immunodeficient rats. The presence of high density DCX+ grafts (green) in the center of the ventral horn and along the cell injection tract was seen (Fig. 4A, B). The identity of DCX expressing grafted human neurons was confirmed by co-staining with human-specific nuclear antibody (hNUMA). Virtually all hNUMA+ cells showed

◀**Fig. 2** DCX expression in developing rat spinal cord. **A**–**A′** Transverse spinal cord section taken from 21-day-old rat fetus and stained with DCX and NeuN antibody. An intense DCX immunoreactivity distributed between the laminae I–V can be seen (**A**). At the base of the ventral horn occasional solitary DCX-IR interneurons can be identified (**A′**; *yellow arrow*). **B**–**B″** At postnatal day 5, DCX immunoreactive neurons were identified primarily in the dorsal horn and in medial regions of laminae I–V (**B**, **B′**; *white arrows*). A comparable DCX expression in the corticospinal tract can also be seen (**B**; CST). In the ventral horn, the majority of NeuN+ neurons were DCX negative (**B″**; *white arrows*). **C**–**C″** In 20-day-old rats, DCX immunoreactivity was confined to neurons localized in the superficial laminae of the dorsal horn (I–III) and to the corticospinal tract (*CST* corticospinal tract; *white arrows*). **D**–**D″** Transverse spinal cord sections taken from 1-day-old rat pup and stained with GFAP and vimentin antibody. Mature GFAP+ astrocytes localized primarily at the periphery of the white matter can be identified (**D**). In contrast, dense networks of immature vimentin+ glial cells in the same region can be seen (**D′**, **D″**). **E** Transverse spinal cord sections taken from 3-month-old adult rat and stained with GFAP and NeuN antibody. A complete repopulation of the white and gray matter with mature GFAP+ astrocytes can be seen. *Scale bars*: **A**, **C′** = 100 μm; **B**, **C** = 200 μm; **B**, **B′** = 50 μm, **C″** = 1500 μm, **D**-50 μm, **E**-200 μm. *DH* dorsal horn, *CST* corticospinal tract. **F** Western blot analysis of DCX expression in rat and porcine spinal cord. DCX expression in developing spinal cord at various fetal and postnatal developmental stages in pig and rat detected by western blot. DCX intensity was normalized to beta tubulin and plotted as a *bar graph*. Rat and pig fibroblasts were blotted together with pig NSCs to validate goat polyclonal anti-DCX (sc-8066) antibody specificity

also DCX IR (Fig. 4A′ B′, B″; white arrows). In addition, extensive sprouting of DCX+ processes derived from grafted neurons and projecting toward endogenous NeuN+ neurons was also seen (Fig. 4A′, B′, B″; yellow arrows).

Porcine iPS-NSCs transplanted into the ventral lumbar spinal cord in immunosuppressed naive pigs showed intense DCX expression at 4 weeks after transplantation with individual grafts easily identified in otherwise DCX negative spinal cord tissue (Fig. 4C; white arrows). The majority of grafted DCX IR neurons were also NeuN positive (Fig. 4C′, C″; white arrows). Numerous DCX positive processes derived from grafted neurons and surrounding NeuN + α-motoneurons (Fig. 4C′, C″; white asterisks) were also seen.

Discussion

Doublecortin Expression in Developing Rat and Porcine Spinal Cord

Consistent with previously published data in rats and chickens (Gleeson et al. 1999), our present data confirmed a transient DCX expression in rat and porcine spinal cord migrating neurons during early and late fetal stage and early postnatal period of spinal cord development. In both species, the majority of neurons in all laminae showed DCX IR during the early fetal stage which was then followed by a progressive loss of DCX IR in the ventral horn, in the intermediate zone and with the last population of neurons which displayed DCX expression being neurons localized in superficial DH. The laminar time course of DCX expression, i.e., initial general DCX expression in all neuronal populations and then progressive loss of DCX expression from ventral horn toward DH, appears to follow the time course of neurogenesis/maturation in the developing spinal cord. These studies, using [3H]thymidine autoradiography in developing rat spinal cord, show that the motoneuronal pools in the ventral horn undergo final mitosis between 11 and 13 days of gestation, followed by neurons in the intermediate zone on days 12–15 and then by neurons in substantia gelatinosa between days 14–16 (Nornes and Das 1974).

However, interestingly, by comparing the time course of DCX expression between rats and pigs, a substantially different pattern was seen. In porcine spinal cord, DCX neuronal expression occurred only during the fetal stage, but no DCX expression was identified in newborn piglets, while a clear DCX IR in superficial DH was still seen in 20-day-old rats. The differential time course of DCX expression between these 2 animal species is likely related to a much more advanced neuronal maturation seen in newborn piglets and which correlates with fully developed ambulatory functions on postnatal day one. In contrary to piglets, the locomotor movement of newborn rats is limited within the first postnatal week.

Doublecortin Expression in In Vitro-Induced NSCs and in Spinally Grafted Human ES-NSCs and Porcine iPS-NSCs

In our previous in vitro studies, we have reported on DCX expression in human embryonic stem cells (ES) and human induced pluripotent stem cell (hiPSC)-derived NSCs differentiated in vitro for 4 weeks (Yuan et al. 2011) as well as in human fetal tissue-derived spinal stem cells at 3 weeks after in vitro differentiation (Usvald et al. 2010). These in vitro data are consistent with the reported DCX expression in cultured early postmitotic rat neurons (Gleeson et al. 1999) and brain-derived porcine neuronal precursors (Schwartz et al. 2005).

In our current study, a similar DCX expression pattern was seen in spinally grafted ES-NSCs and porcine iPS-NSCs. Thus, in both cell lines an intense DCX expression was seen at 3–4 weeks after grafting, clearly delineating the population of grafted cells once grafted into mature otherwise DCX negative spinal cord tissue.

In our previous studies, we have demonstrated continuing DCX expression in human spinal stem cell-derived

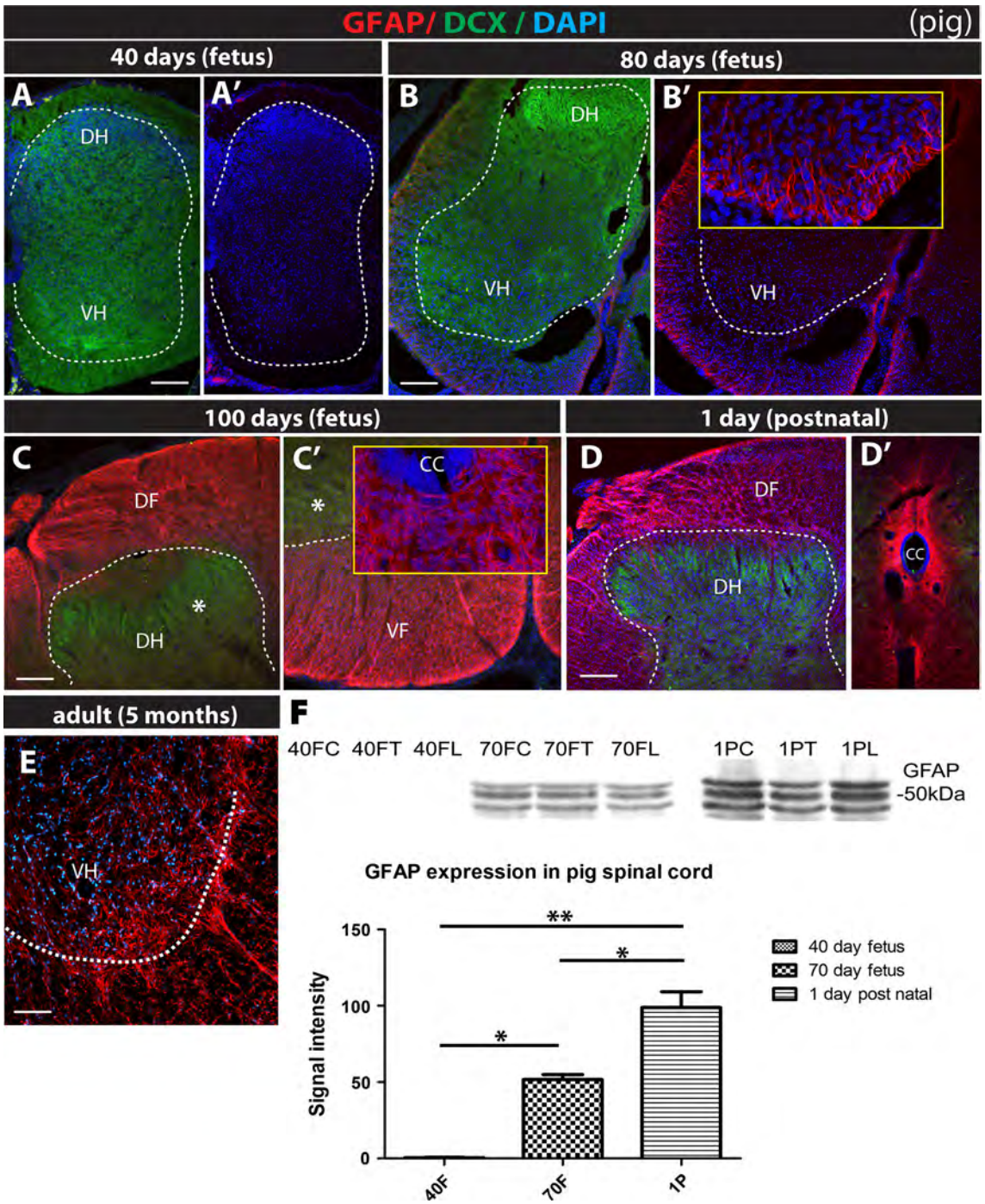

Fig. 3 Immunohistochemistry of GFAP expression in developing porcine spinal cord. No GFAP (*red*) immunoreactivity in the lumbar spinal cord was seen in 40-day-old fetus (**A**–**A**′). At 80 days, a radial type of GFAP positive astrocytes localized in the subpial regions and extending GFAP+ processes toward deeper layers of the white matter can be seen (**B**, **B**′). In 100-day-old fetus and 1-day-old piglet, the *white matter* in dorsal and ventral funiculi showed an intense GFAP immunoreactivity with a clearly delineated GFAP+ network of astrocyte processes (**C**–**D**). In adult 5-month-old pig, a complete repopulation of white matter and gray matter with GFAP+ astrocytes can be seen (**E**). *Scale bars* **A**, **B** = 500 μm; **C**, **D**, **E** = 200 μm. *DH* dorsal horn, *VH* ventral horn, *DF* dorsal funiculus, *CC* central canal. **F** Western blot analysis of GFAP expression in porcine spinal cord. GFAP expression in developing spinal cord at various fetal and postnatal developmental stages in pig detected by western blot. Statistical analysis of three technical replicates per sample by 1-way Anova ($p = 0.0013$) with Bonferronis multiple comparison test confirmed that GFAP protein expression in spinal cord of 40-day-old fetus, 70-day-old fetus, and 1-day-old newborn is significantly different. Abbreviations: *FC* fetal cervical segment, *FT* fetal thoracic segment, *FL* fetal lumbar segment, *1PC* first postnatal day cervical segment, *1PT* first postnatal day thoracic segment, *1PL* first postnatal day lumbar segment

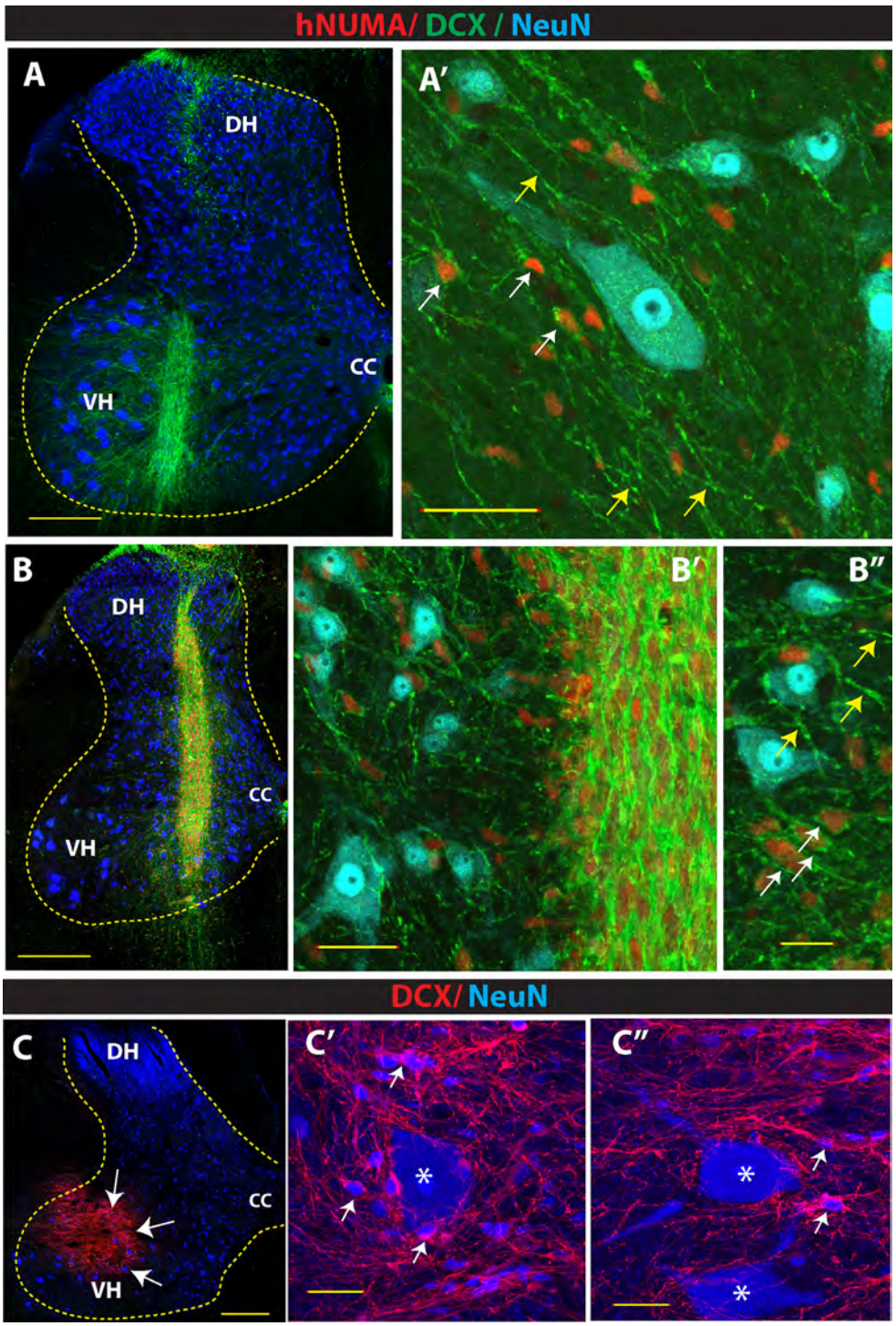

Fig. 4 DCX expression in spinally grafted human ES-derived and porcine iPS-derived neural precursors. Intense DCX expression in human ES-NSCs grafted into the lumbar spinal cord of immunodeficient rats was seen at 3 weeks after grafting (**A**, **B**). The DCX expression was only seen in grafted human neurons expressing a human-specific nuclear protein (hNUMA), (**A′**, **B′**). A high density DCX positive network of neuronal dendrites can also be seen (**A′**, **B″**). A comparable level of DCX expression in spinally grafted porcine iPS-NSCs was seen at 4 weeks after grafting in continuously immunosuppressed pigs (**C**). The majority of grafted cells showed neuronal differentiation (NeuN) and extensive axo-dendritic arborization of DCX+ processes (**C′**, **C″**; *white arrows*) surrounding a large host α-motoneurons (**C′**, **C″**; *white asterisks*). *Scale bars*: **A**, **B**, **C** = 500 µm; **A′**, **B′**, **B″** = 100 µm, **C′**, **C″** = 50 µm. *DH* dorsal horn, *VH* ventral horn, *CC* central canal

neurons at 3 weeks–3 months after grafting when cells were grafted into the lumbar spinal cord in mature SOD1^{G93A} rats, mature SD rats with spinal ischemic injury or in mature naïve pigs (Hefferan et al. 2012; Cizkova et al. 2007; Usvald et al. 2010). However, at 3 months after grafting into the spinal cord of mature SD rats with spinal ischemic injury, an intense NSE (neuron-specific enolase; mature neuronal marker) was already seen and was particularly expressed in neurons with very weak or no DCX IR. These data demonstrate that, depending on the stage when NSCs are grafted in vivo (i.e., proliferating or previously in vitro-induced NSCs) periods of 3 months or longer will be required for full neuronal maturation and loss of DCX IR. This is consistent with our recent observation confirming that no DCX IR is present in human ES-NSCs at 8 months after grafting into the lumbar spinal cord of immunodeficient rats (unpublished observation).

Differentiation of DCX Expression in Grafted Versus Host Neurons

As we have demonstrated, DCX expression in the developing rat spinal cord is no longer present in animals older than 4 weeks and is absent in newborn piglets. Therefore, the presence of DCX positive neurons seen in spinally grafted adult rats or minipigs can reliably be used to identify grafted terminally differentiated neurons. While spinal grafting of neural precursors can potentially stimulate proliferation of endogenous neuronal precursors and lead to a false DCX IR, at present there is no evidence that neurogenesis is taking place in adult naive or injured rat spinal cord (Horner et al. 2000; Yang et al. 2006). In addition, in the absence of any cell labeling (such as GFP), DCX expression in grafted neurons of human origin can be validated further by co-staining with several human-specific antibodies. As shown in the previous and our current study (Usvald et al. 2010; Kakinohana et al. 2012), the use of NUMA antibody is optimal to identify colocalization with DCX expression, particularly when clear DCX expression in neuronal soma is present. Second, for more discrete structures such as DCX+ axons or dendrites, the use of human-specific synaptophysin appears to provide a reliable marker. As we have shown previously, a clear spatial colocalization of hSYN+ punctata with DCX+ processes was identified in grafted human neurons in porcine spinal cord using confocal images acquired with 0.3 μm optical Z resolution (Usvald et al. 2010).

Astrocyte GFAP Expression in Developing Porcine Spinal Cord

Considering the DCX expression profile observed in this study, it has been demonstrated that the maturation of spinal cord (and brain) neurons spatially coincides with astrocyte maturation as evidenced by the presence of GFAP immunoreactive cells. Accordingly, in 1-day-old porcine spinal cord, a well developed and dense GFAP+ astrocyte network was already seen in white and in part in gray matter which contrasted with a well documented lack of GFAP+ astrocytes in the white and gray matter in newborn rats. It was also demonstrated that the expression of vimentin (a glial precursor marker) seen in newborn rats is progressively replaced by GFAP IR during the first 3 postnatal weeks (Oudega and Marani 1991; Hirano and Goldman 1988). These data are consistent with our current observation, which demonstrate intense vimentin staining in white and gray matter of P0 rat pups. By Western blot analysis, we have also confirmed that the GFAP expression is first seen around 70–80th fetal day in minipigs, (i.e., approximately half of the gestation time in pigs), which is in contrast to the first observation of GFAP expression seen at E18 in rats (Oudega and Marani 1991).

Summary

In the present study, we characterized the time course of DCX and GFAP expression in developing rat and porcine spinal cord.

In contrast to rats, which display continuing spinal neuronal expression of DCX for the first 21 postnatal days, no DCX expression was seen in newborn piglets. In both adult rats and pigs, no DCX was identified. GFAP expression started around 70–80th fetal day in miniature pig spinal cord, suggesting earlier maturation of the CNS in minipigs in comparison to rodents. This data indicates that in spinal grafting studies which employ a postnatal or adult porcine model, the expression of DCX can be used as a reliable marker of grafted neurons of rodent, human or even pig origin. In contrast, if grafted neurons are to be analyzed during the first 4 postnatal weeks in the rat spinal cord, additional markers or cell-specific labeling of grafted cells need to be employed to identify reliably grafted early postmitotic neurons and to differentiate the DCX expression from the neurons of the host.

Acknowledgments This study was funded by CIRM (M.M.), TA01011466, CZ.1.05./2.1.00/03.0124, and RVO: 67985904 (J.J., S.J., J.M., J.S., M.H.).

References

Cao QL, Onifer SM, Whittemore SR (2008) Labeling stem cells in vitro for identification of their differentiated phenotypes after grafting into the CNS. Methods Mol Biol 438:361–374

Cizkova D, Rosocha J, Vanicky I, Jergova S, Cizek M (2006) Transplants of human mesenchymal stem cells improve functional recovery after spinal cord injury in the rat. Cell Mol Neurobiol 26(7–8):1165–1178

Cizkova D, Kakinohana O, Kucharova K, Marsala S, Johe K, Hazel T, Hefferan MP, Marsala M (2007) Functional recovery in rats with ischemic paraplegia after spinal grafting of human spinal stem cells. Neuroscience 147(2):546–560. doi:10.1016/j.neuroscience.2007.02.065

Couillard-Despres S, Winner B, Schaubeck S, Aigner R, Vroemen M, Weidner N, Bogdahn U, Winkler J, Kuhn HG, Aigner L (2005) Doublecortin expression levels in adult brain reflect neurogenesis. Eur J Neurosci 21(1):1–14

Couillard-Despres S, Finkl R, Winner B, Ploetz S, Wiedermann D, Aigner R, Bogdahn U, Winkler J, Hoehn M, Aigner L (2008) In vivo optical imaging of neurogenesis: watching new neurons in the intact brain. Mol Imaging 7(1):28–34

Darsalia V, Kallur T, Kokaia Z (2007) Survival, migration and neuronal differentiation of human fetal striatal and cortical neural stem cells grafted in stroke-damaged rat striatum. Eur J Neurosci 26(3):605–614

Dolezalova D, Hruska-Plochan M, Bjarkam CR, Sorensen JC, Cunningham M, Weingarten D, Ciacci JD, Juhas S, Juhasova J, Motlik J, Hefferan MP, Hazel T, Johe K, Carromeu C, Muotri A, Bui J, Strnadel J, Marsala M (2014) Pig models of neurodegenerative disorders: utilization in cell replacement-based preclinical safety and efficacy studies. J Comp Neurol. doi:10.1002/cne.23575

Englund U, Bjorklund A, Wictorin K (2002) Migration patterns and phenotypic differentiation of long-term expanded human neural progenitor cells after transplantation into the adult rat brain. Brain Res Dev Brain Res 134(1–2):123–141

Gleeson JG, Lin PT, Flanagan LA, Walsh CA (1999) Doublecortin is a microtubule-associated protein and is expressed widely by migrating neurons. Neuron 23(2):257–271

Hakamata Y, Tahara K, Uchida H, Sakuma Y, Nakamura M, Kume A, Murakami T, Takahashi M, Takahashi R, Hirabayashi M, Ueda M, Miyoshi I, Kasai N, Kobayashi E (2001) Green fluorescent protein-transgenic rat: a tool for organ transplantation research. Biochem Biophys Res Commun 286(4):779–785

Hefferan MP, Galik J, Kakinohana O, Sekerkova G, Santucci C, Marsala S, Navarro R, Hruska-Plochan M, Johe K, Feldman E, Cleveland DW, Marsala M (2012) Human neural stem cell replacement therapy for amyotrophic lateral sclerosis by spinal transplantation. PLoS One 7(8):e42614. doi:10.1371/journal.pone.0042614

Hirano M, Goldman JE (1988) Gliogenesis in rat spinal cord: evidence for origin of astrocytes and oligodendrocytes from radial precursors. J Neurosci Res 21(2–4):155–167. doi:10.1002/jnr.490210208

Horner PJ, Power AE, Kempermann G, Kuhn HG, Palmer TD, Winkler J, Thal LJ, Gage FH (2000) Proliferation and differentiation of progenitor cells throughout the intact adult rat spinal cord. J Neurosci 20(6):2218–2228

Hua R, Doucette R, Walz W (2008) Doublecortin-expressing cells in the ischemic penumbra of a small-vessel stroke. J Neurosci Res 86(4):883–893

Inoue H, Ohsawa I, Murakami T, Kimura A, Hakamata Y, Sato Y, Kaneko T, Takahashi M, Okada T, Ozawa K, Francis J, Leone P, Kobayashi E (2005) Development of new inbred transgenic strains of rats with LacZ or GFP. Biochem Biophys Res Commun 329(1):288–295

Jin K, Zhu Y, Sun Y, Mao XO, Xie L, Greenberg DA (2002) Vascular endothelial growth factor (VEGF) stimulates neurogenesis in vitro and in vivo. Proc Natl Acad Sci USA 99(18):11946–11950

Johansson CB, Momma S, Clarke DL, Risling M, Lendahl U, Frisén J (1999) Identification of a neural stem cell in the adult mammalian central nervous system. Cell 96(1):25–34

Kakinohana O, Cizkova D, Tomori Z, Hedlund E, Marsala S, Isacson O, Marsala M (2004) Region-specific cell grafting into cervical and lumbar spinal cord in rat: a qualitative and quantitative stereological study. Exp Neurol 190(1):122–132. doi:10.1016/j.expneurol.2004.07.014

Kakinohana O, Juhasova J, Juhas S, Motlik J, Platoshyn O, Galik J, Hefferan M, Yuan SH, Vidal JG, Carson CT, van Gorp S, Goldberg D, Leerink M, Lazar P, Marsala S, Miyanohara A, Keshavarzi S, Ciacci JD, Marsala M (2012) Survival and differentiation of human embryonic stem cell-derived neural precursors grafted spinally in spinal ischemia-injured rats or in naive immunosuppressed minipigs: a qualitative and quantitative study. Cell Transpl 21(12):2603–2619. doi:10.3727/096368912X653200

Karl C, Couillard-Despres S, Prang P, Munding M, Kilb W, Brigadski T, Plotz S, Mages W, Luhmann H, Winkler J, Bogdahn U, Aigner L (2005) Neuronal precursor-specific activity of a human doublecortin regulatory sequence. J Neurochem 92(2):264–282

Kawaguchi A, Miyata T, Sawamoto K, Takashita N, Murayama A, Akamatsu W, Ogawa M, Okabe M, Tano Y, Goldman SA, Okano H (2001) Nestin-EGFP transgenic mice: visualization of the self-renewal and multipotency of CNS stem cells. Mol Cell Neurosci 17(2):259–273

Kelly S, Bliss TM, Shah AK, Sun GH, Ma M, Foo WC, Masel J, Yenari MA, Weissman IL, Uchida N, Palmer T, Steinberg GK (2004) Transplanted human fetal neural stem cells survive, migrate, and differentiate in ischemic rat cerebral cortex. Proc Natl Acad Sci USA 101(32):11839–11844

Lepore AC, Fischer I (2005) Lineage-restricted neural precursors survive, migrate, and differentiate following transplantation into the injured adult spinal cord. Exp Neurol 194(1):230–242

Lu P, Wang Y, Graham L, McHale K, Gao M, Wu D, Brock J, Blesch A, Rosenzweig ES, Havton LA, Zheng B, Conner JM, Marsala M, Tuszynski MH (2012) Long-distance growth and connectivity of neural stem cells after severe spinal cord injury. Cell 150(6):1264–1273. doi:10.1016/j.cell.2012.08.020

Magavi SS, Macklis JD (2008) Immunocytochemical analysis of neuronal differentiation. Methods Mol Biol 438:345–352

Marchetto MC, Carromeu C, Acab A, Yu D, Yeo GW, Mu Y, Chen G, Gage FH, Muotri AR (2010) A model for neural development and treatment of Rett syndrome using human induced pluripotent stem cells. Cell 143(4):527–539. doi:10.1016/j.cell.2010.10.016

Marsala M, Kakinohana O, Yaksh TL, Tomori Z, Marsala S, Cizkova D (2004) Spinal implantation of hNT neurons and neuronal precursors: graft survival and functional effects in rats with ischemic spastic paraplegia. Eur J Neurosci 20(9):2401–2414. doi:10.1111/j.1460-9568.2004.03702.x

Nacher J, Crespo C, McEwen BS (2001) Doublecortin expression in the adult rat telencephalon. Eur J Neurosci 14(4):629–644

Nornes HO, Das GD (1974) Temporal pattern of neurogenesis in spinal cord of rat. I. An autoradiographic study–time and sites of origin and migration and settling patterns of neuroblasts. Brain Res 73(1):121–138

Okabe M, Ikawa M, Kominami K, Nakanishi T, Nishimune Y (1997) 'Green mice' as a source of ubiquitous green cells. FEBS Lett 407(3):313–319

Oudega M, Marani E (1991) Expression of vimentin and glial fibrillary acidic protein in the developing rat spinal cord: an immunocytochemical study of the spinal cord glial system. J Anat 179:97–114

Sabelström H, Stenudd M, Frisén J (2014) Neural stem cells in the adult spinal cord. Exp Neurol 260:44–49. doi:10.1016/j.expneurol.2013.01.026

Schwartz PH, Nethercott H, Kirov II, Ziaeian B, Young MJ, Klassen H (2005) Expression of neurodevelopmental markers by cultured porcine neural precursor cells. Stem Cells 23(9):1286–1294. doi:10.1634/stemcells.2004-0306

Sevc J, Goldberg D, van Gorp S, Leerink M, Juhas S, Juhasova J, Marsala S, Hruska-Plochan M, Hefferan MP, Motlik J, Rypacek

F, Machova L, Kakinohana O, Santucci C, Johe K, Lukacova N, Yamada K, Bui JD, Marsala M (2013) Effective long-term immunosuppression in rats by subcutaneously implanted sustained-release tacrolimus pellet: effect on spinally grafted human neural precursor survival. Exp Neurol 248:85–99. doi:10.1016/j.expneurol.2013.05.017

Tabar V, Panagiotakos G, Greenberg ED, Chan BK, Sadelain M, Gutin PH, Studer L (2005) Migration and differentiation of neural precursors derived from human embryonic stem cells in the rat brain. Nat Biotechnol 23(5):601–606

Usvald D, Vodicka P, Hlucilova J, Prochazka R, Motlik J, Strnadel J, Kucharova K, Johe K, Marsala S, Scadeng M, Kakinohana O, Navarro R, Santa M, Hefferan MP, Yaksh TL, Marsala M (2010) Analysis of dosing regimen and reproducibility of intraspinal grafting of human spinal stem cells in immunosuppressed minipigs. Cell Transpl 19:1103–1122. doi:10.3727/096368910X503406

van Gorp S, Leerink M, Kakinohana O, Platoshyn O, Santucci C, Galik J, Joosten EA, Hruska-Plochan M, Goldberg D, Marsala S, Johe K, Ciacci JD, Marsala M (2013) Amelioration of motor/sensory dysfunction and spasticity in a rat model of acute lumbar spinal cord injury by human neural stem cell transplantation. Stem Cell Res Ther 4(5):57. doi:10.1186/scrt209

Walker TL, Yasuda T, Adams DJ, Bartlett PF (2007) The doublecortin-expressing population in the developing and adult brain contains multipotential precursors in addition to neuronal-lineage cells. J Neurosci 27(14):3734–3742

Wallace PK, Muirhead KA (2007) Cell tracking 2007: a proliferation of probes and applications. Immunol Invest 36(5–6):527–561

Yang H, Lu P, McKay HM, Bernot T, Keirstead H, Steward O, Gage FH, Edgerton VR, Tuszynski MH (2006) Endogenous neurogenesis replaces oligodendrocytes and astrocytes after primate spinal cord injury. J Neurosci 26(8):2157–2166. doi:10.1523/JNEUROSCI.4070-05.2005

Yuan SH, Martin J, Elia J, Flippin J, Paramban RI, Hefferan MP, Vidal JG, Mu Y, Killian RL, Israel MA, Emre N, Marsala S, Marsala M, Gage FH, Goldstein LS, Carson CT (2011) Cell-surface marker signatures for the isolation of neural stem cells, glia and neurons derived from human pluripotent stem cells. PLoS One 6(3):e17540. doi:10.1371/journal.pone.0017540